suggested [268], its signal in the electron density map could be overshadowed by the contribution of the nearby electron-rich Mn/Ca ions. Nevertheless, assuming that this Cl^- could also be exchanged against Br^-, this very close distance would contradict the EXAFS results on Br^- exchanged PSII from spinach [264] that suggested a $Cl^-\cdots water\cdots Mn_4Ca$ model with a distance of ca 5 Å between Cl^- and Mn/Ca.

3.2.4 Chlorophylls

To maintain solar energy conversion, an appropriate cofactor able to absorb and to transmit energy is essential. In PSII this role is assigned to Chl *a*, tetrapyrrol derivative with cyclic π-electron system and phytol tail attached to the propionate group (Fig. 3). They are divided into two unequal classes: the majority of Chl *a* molecules are involved in actual light absorption and transfer of excited electron state, termed exciton, and the minority is responsible for photochemical reactions and electron transfer (see section 1.2 for details).

All light absorbing Chl *a* are found within two antenna subunits CP43 and CP47 (see section 3.1.1.2), and serve as protein matrix for optimal arrangement of chlorophyll molecules. Each subunit harbours 16 and 13 Chl *a*, respectively (in contrast to the model at 3.5 Å [255] where one additional Chl *a* was erroneously assigned to CP43 subunit, the refined structure at 2.9 Å resolution confirmed clearly that this space is filled with a tightly bound DGDG lipid), organized in a distinct bilayer structure – with one layer close to the lumen and other to the cytoplasmic site of the membrane. Interestingly, the cytoplasmic layer is more chlorophyll-rich and comprises nine Chl *a* molecules in both subunits related by the local pseudo C_2 (Fe^{2+}) symmetry while at the lumenal site there are only four and seven molecules in CP43 and CP47, respectively (see also section 3.1.1.2). The electron density at 2.9 Å resolution allowed the complete modelling of phytol chains for all 35 chlorophyll molecules (see example in Fig. 49).

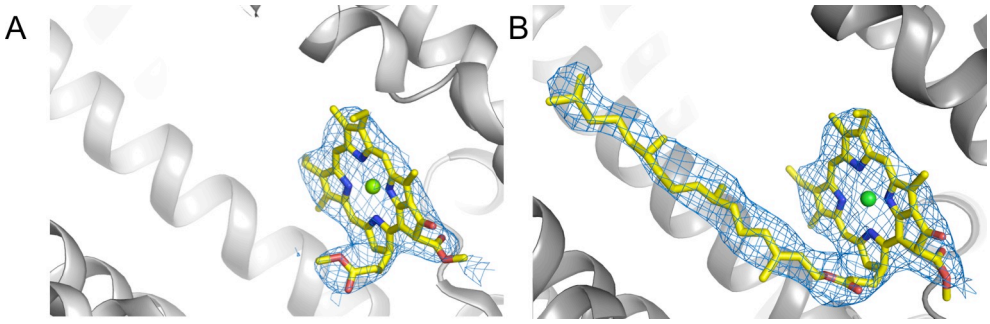

Figure 49. Improved quality of the electron density at 2.9 Å resolution. (a) Electron density (blue, with contour level 1.2σ) for Chl37 (yellow), embedded in (grey) at 3.0 Å resolution (pdb code 2AXT). The phytol chain could

not be traced because of the poor quality of the electron density. (b) Nearly the same view as in panel a, electron density at 1.2σ level of the same Chl37 at 2.9 Å resolution, the phytol chain could be traced completely (pdb code 3BZ1).

3.2.5 Carotenoids

Carotenoids are chromophors containing an almost linear chain of conjugated double bonds (Fig. 3 and section 1.2). In PSII they play a predominant role in quenching of triplet states of Chl *a* molecules by means of rapid triplet-triplet transfer, and might participate in excitation energy transfer as many of them are at van der Waals contacts with neighbouring Chl *a* molecules or with other carotenoids (Fig. 50).

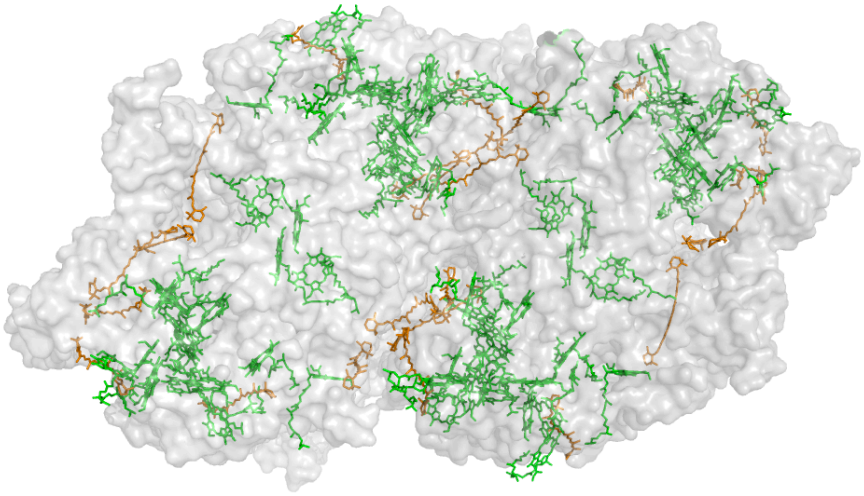

Figure 50. Carotenoid-chlorophyll interactions. View from the cytoplasmic side. PSII is shown as grey transparent surface, whereas chlorophylls (green) and carotenoids (orange) are shown as stick models.

Interestingly in the 2.9 Å resolution model an additional carotenoid molecule (Car15) was found on the D2 side in close vicinity to Car_{D2}, although in a shifted position in comparison with Car53 modelled at 3.5 Å resolution [255]. Car15 is located at van der Waals distance (3.4 Å) to Car12 and at van der Waals distance (4.1 Å) to Car_{D2}. Carotenoids Car_{D2}, Car12, Car13, Car16 and Car15 are all at van der Waals distance next to each other and possibly coupled for fast electron/exciton transfer.

Additionally, clustered carotenoids (Car3, 4, 5, 6) are might be involved in solar energy absorption and broaden the absorption spectrum, thereby improving the overall efficiency of PSII.

3.3 Channels

Since water is the substrate of OEC and the side product (O_2) is potentially harmful [269, 270], the efficient catalysis of PSII requires streamlined delivery of the educt (H_2O) to and removal of products (electrons, O_2, protons) from the Mn_4Ca cluster.

The presence of a specific channel for oxygen removal from the OEC to avoid oxidative damage of PSII was first postulated by Anderson [271].

Based on the first crystal structure of PSII at 3.8 Å resolution [272], it was suggested that the membrane-extrinsic subunit PsbO with its tube-like structure could serve such a function in product and educt transport [273]. With the improvement of crystal structures at 3.5 Å [255] and 3.0 Å resolution [41], more detailed analyses of possible channels for water and oxygen transfer became feasible. Using different approaches, several groups suggested a rather complex transport network consisting of three to four channels formed by various subunits in PSII [274-279].

Calculations with the improved model at 2.9 Å resolution revealed a higher number of substrate and product channels in comparison to previous studies [274, 275]. In total, nine distinct channels connecting the Mn_4Ca cluster with the lumen were identified; two of them being possible pathways for water, two for oxygen, and five being putative proton exit pathways. The found channels were also verified with data from crystal structures of PSII derivatized with Xe and Kr.

3.3.1 Theoretical calculations

In total, more than 80 possible trajectories of channels were calculated using the program CAVER [128] starting from several different origins that cover the area of the Mn_4Ca cluster and with various grid sizes in the range of 0.4 – 0.6 Å. The most probable trajectories were assigned on the basis of several criteria like channel diameter, length, hydrophobicity, and the physical and chemical properties of the transported molecules and merged by their similarity into two channels for water, one for oxygen and five for proton transport (Figs. 51, 52).

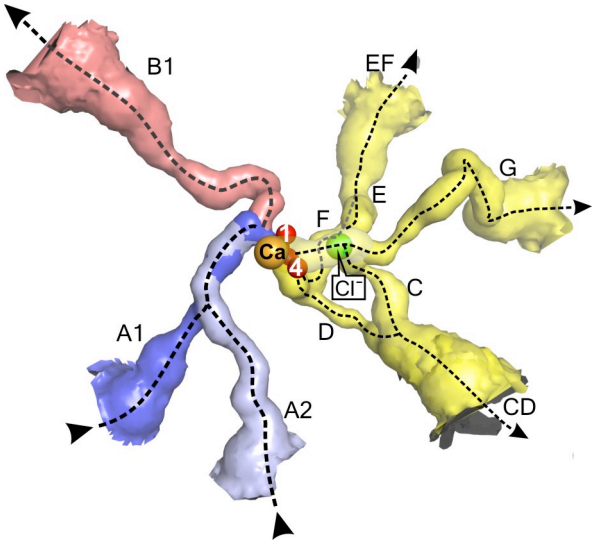

Figure 51. Calculated channels in PSII. View from the stromal side onto the membrane plane showing the Mn_4Ca cluster (only Ca (orange sphere), Mn1 and Mn4 (red spheres) are visible), the chloride ion (Cl^-, green sphere) and putative channels connecting the cluster to the lumenal side. Water/oxygen channels are in blue (A1), light blue (A2) and red (B1), possible proton channels (C to G) are in yellow.

The assignment of channels was made based on the following assumptions: the radius of the water channel has to be greater than 1.49 ± 0.26 Å, where 1.49Å is the radius of water [68] and 0.26 Å is the estimated maximal coordinate error calculated by SFCHECK [130] for the obtained crystal structure of PSII at 2.9 Å resolution. The oxygen channel must be the widest (because the radius for oxygen is 1.52 Å (2.13 Å along the O=O bond)), the most hydrophobic (as oxygen is hydrophobic) and desirably the shortest (to provide fast oxygen removal from the Mn_4Ca cluster). Regarding the proton channels, the length at the bottleneck (channel narrows) was taken as the most significant parameter (must not be longer than the maximal length of a hydrogen bond, 3.5 Å ± 0.26 Å). In terms of the radius all channels, which are not wide enough for water or oxygen transport (radii below 1.49 Å ± 0.26 Å), but still capable of accommodating water molecules, were postulated as possible proton channels (Fig. 52).

Channels A1 and A2 (Figs. 51, 52) most probably play the leading role in the water supply from the lumen to the Mn_4Ca cluster. Both channels originate at the lumenal surface of subunits CP43 and D1 with their entrances being ca. 15 Å apart and join at the distance of ca. 14 Å from the Mn_4Ca cluster. The lengths of the channels are roughly 25 Å and 35 Å with minimal radii of 1.24 Å and 1.38 Å for A1 and A2, respectively.

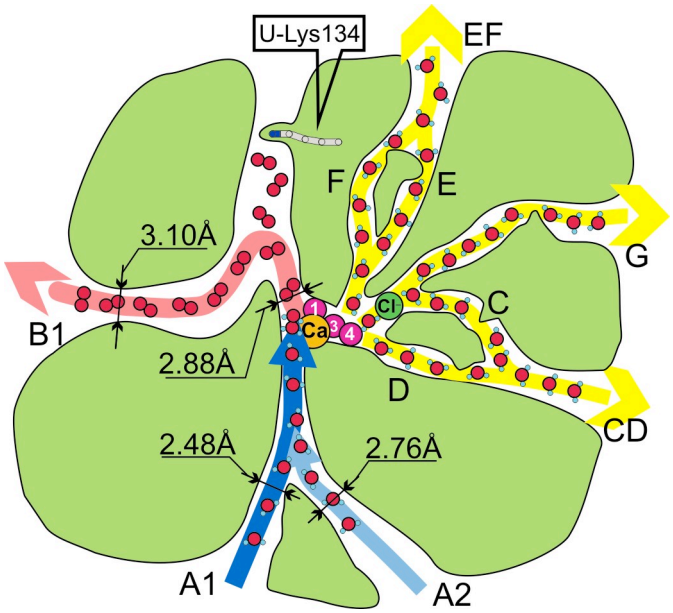

Figure 52. Schematic view (same view direction as in Fig. 51) of possible substrate and product channels in PSII. Minimum diameters of the water/oxygen channels (in Å) are indicated by black arrows. Thick coloured arrows indicate the suggested paths for water supply (blue), oxygen (red) and proton (yellow) removal. Note U-Lys134 from subunit PsbU that closes a side-exit of channel B1 and could open it by a conformational change, *vide infra*.

The channels are formed mainly by residues of subunits D1 and CP43 as well as by head groups of lipids DGDG1 and DGDG2. The amount of polar residues forming the walls of channel A1 is 26, and that of non-polar (hydrophobic) residues is 28, but the ratio between them is dependent on their position along the channel – there is a gradual increase of non-polar (hydrophobic) groups towards the Mn_4Ca cluster. At the channel entrance near the lumen, polar (hydrophilic) groups predominate (up to 85%), whereas near the Mn_4Ca cluster only 40% of the atoms belong to polar groups. A similar decrease of polarity from the lumen towards the Mn_4Ca cluster is observed along channel A2 (see Appendix Table 7.7).

The only channel found to be suitable for oxygen removal from the Mn_4Ca cluster is channel B1. It is ~33.5 Å long and leads away from the Mn_4Ca cluster starting at Ca, Mn1 and Mn2 atoms. This channel is formed by residues of subunits D1, CP43 and *cyt c-550*, and its surface is lined mainly with non-polar (hydrophobic) groups (ca. 60% of all the contributing atoms). Although this channel is not the shortest one, its minimal radius of 1.44 Å renders it the best candidate for easy diffusion of oxygen.

The profile of channel B1 features a sharp turn (Fig. 52), where a possible accumulation of oxygen molecules could occur. Interestingly, this turn is separated from the lumen only by the side chain of the C-terminal Lys134 from subunit PsbU (U-Lys134). The

side chain of this residue is held in this position by one salt bridge formed with Asp79 from subunit PsbV (U-Lys134NZ ··· OD2Asp79-V, 3.26Å), whereas there is no strong hydrogen bond to the terminal carboxylate group of PsbU (the closest interactions are U-Lys134OXT ··· NH2Arg384-D (4.35 Å) and U-Lys134O ··· NH1Arg384-D (3.57 Å), (see Fig. 53)), but it can not be excluded that water molecule(s) mediate(s) these long hydrogen bonds.

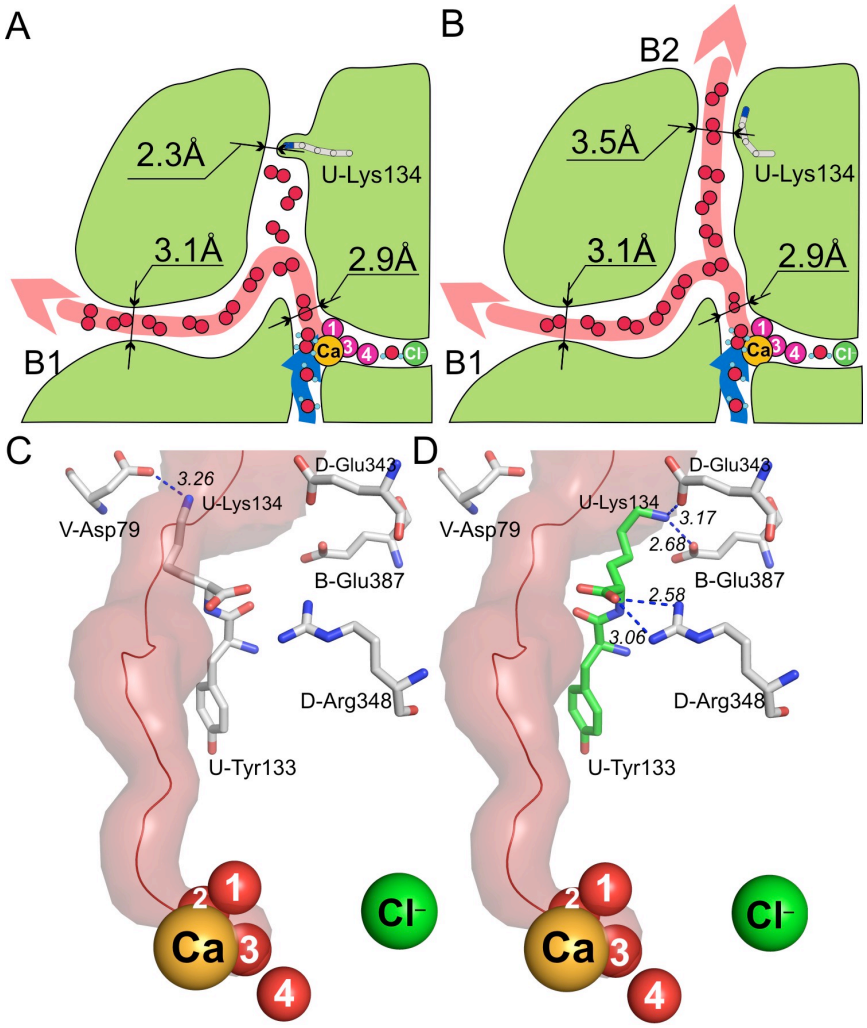

Figure 53. Scheme of activation of the second possible oxygen channel B2. Minimum diameters of the oxygen channels (in Å) are indicated by black arrows. Thick coloured arrows indicate the suggested paths for water supply to (blue, channel A1) and oxygen removal (red, channels B1, B2) from the Mn_4Ca cluster. (A) Channel B2 is closed by U-Lys134; (B) Channel B2 is open after conformational change of U-Lys134; (C) View of closed conformation of U-Lys134 grey – "closed"; (D) View of open conformation of U-Lys134 green – "open".

To evaluate the possibility of additional channel formation, the conformation of U-Lys134 was changed manually in COOT [122], and 50 cycles of "model_minimize" procedure for the energy minimization excluding phase information (solvent free structure idealization) in CNS 1.2 was performed [117]. In the new position, U-Lys134 has comparable

stereochemical properties as in the original position, and forms new putative hydrogen bonds U-Lys134NZ ··· OE1Glu387-B (2.68 Å), U-Lys134NZ ··· OE1Glu343-D (3.17 Å) and U-Lys134OXT ··· NH1Arg348-D (2.58 Å). This conformational change is associated with the opening of an additional putative oxygen channel, termed B2 (Figs. 52, 53), with minimal radius of 1.75 Å, length of 29.5 Å and with predominance of hydrophobic residues at its surface (see Appendix Table 7.7).

The finding that channel B2 is only blocked by U-Lys134 and wide enough for oxygen transport is intriguing. Indeed, a simple conformational change, in which one hydrogen bond is replaced by two possible others, is sufficient to open this channel (Fig. 53). To check the relevance of this finding, PsbU amino acid sequences of 40 species of cyanobacteria and two species of red algae were analyzed. Those sequences that show at least 85% homology in the 80 C-terminal residues with PsbU from *T. elongatus*, which presumably have a similar tertiary structure were chosen. This list revealed that at the C-terminal position, four sequences have Lys134 and 22 have Arg134 (9.5 and 52.4%, respectively). Since Arg134 can form hydrogen bonds like Lys134, it could open channel B2 in the same way. Of the remaining 16 sequences, 11 (26.2%) terminate at Tyr133 and two have Gly134, so that channel B2 would be always open. Asp134 is found in three (7.1%) cases, and here the accessibility of channel B2 is not clear.

Okumura et al. [280] investigated the activity of PSII from the red alga *Cyanidium caldarium* reconstituted with mutant PsbU. They showed that mutants lacking the C-terminal Lys exhibit a similar level of oxygen evolution as PSII with full-length wild type PsbU. Provided that the channels are properly formed in the reconstituted samples, this experiment has two possible implications: either channel B2 is irrelevant or U-Lys134 is not a barrier for passing oxygen.

Interestingly, in contrast to the results of [275], water (A1 and A2 defined as ‘back channel’ in [275]) and oxygen channels (B1 and B2 defined as ‘large channel’ in [275]) have contact with Mn1, Mn2, and Ca ions of the OEC. Channels B1 and B2 are wide enough for the passage of methanol (MeOH, radius 1.7 Å [281]), which appears to interact with the Mn_4Ca cluster [282, 283]. Therefore, these channels are possible pathways for MeOH access from the lumen to the OEC. MeOH was suggested to replace substrate water, possibly the one that is less tightly bound to the Mn_4Ca cluster [284-286]. Assuming that MeOH reaches the Mn_4Ca cluster through channels A or B, MeOH most likely binds to Mn1 or Mn2 that are accessible from these channels. Since water approaches Mn_4Ca also from this side, Mn1, Mn2, and Ca are good candidates for the binding of substrate water.

At the other side of the Mn_4Ca cluster, five narrower channels (C, D, E, F and G) start at positions of Mn3 and Mn4 with mostly polar (hydrophilic) groups forming the walls and minimum diameter of 1.3 Å (see Appendix Table 7.7). Channels C and G originate at atom Mn4 and harbour the chloride ion Cl^- (see section 3.2.3), but they have different exits (see Figs. 51, 52, 54).

There is experimental evidence favouring the importance of Cl^- in water oxidation (see review [57]) despite its position at a distance of 6.5 Å from the Mn_4Ca cluster. Notably, Cl^- has been suggested to play a role in proton removal, while being bound to a lysine residue with an anomalously low pKa value [261]. This proposal is in agreement with the range of pKa values for D-Lys317 in the absence of Cl^-, calculated on the basis of the 3.0 Å resolution structure [278], and the present assignment of proton channels. Concerning the mechanism of action of the chloride ion, two (non-exclusive) possibilities are feasible: (i) Cl^- could influence the pKa values of nearby protonatable groups and adjust them for efficient proton transfer away from the OEC, and (ii) a blockage of the channel by Cl^- could prevent leakage of water out of the channels C and G towards the Mn_4Ca cluster and serve to stabilize water chains necessary for proton transfer.

Channels D, E and F initiate at atom Mn3 and diverge, though channels E and F share the same exit to the lumen (EF) (Fig. 54). Similarly, channels C and D unite to channel CD (Fig. 54) and form an exit to the lumen. As mentioned above, all proton channels have short narrow sections that might be filled with fixed water molecules at such positions.

To evaluate the suitability of the narrow channels C-G for proton transfer, water molecules were manually placed inside these channels. In all five channels, it was possible to model water chains with respect to the geometry and presence of donor/acceptor amino acids for proton jumps occurring by the Grotthuss mechanism (proton-hopping) [287, 288]. The proton transfer over long distances is thought to involve a cascade of “hops”, each “hop” relocating a proton via water molecules or protonatable amino acid side chains. This process requires a well-defined orientation of hydrogen bonds and an electrostatic environment that enables transient stabilization of the proton along the transfer pathway.

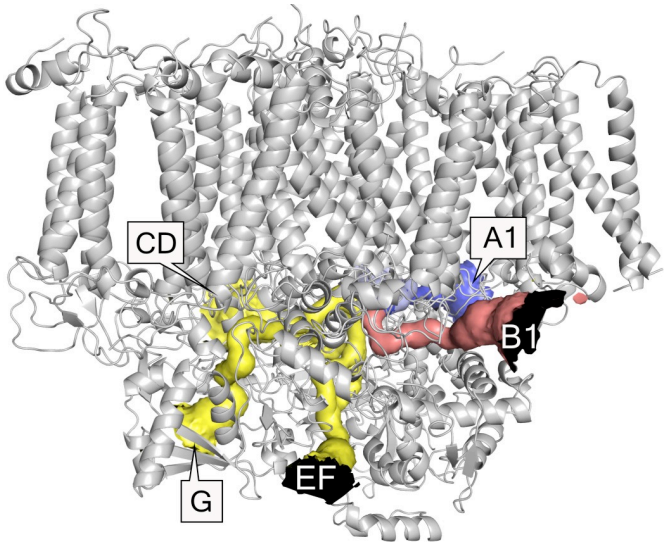

Figure 54. Side view of one PSII monomer along the membrane plane showing openings of the channels towards the lumen. Openings of channels A1, A2 (at the back side, not seen), B1, CD are located close to the membrane surface.

Residue A-Glu65, which has been proposed to be involved in a proton exit pathway [276-278], is located at the bottleneck of channel C. There is enough space within this channel for one water molecule being placed between Cl^- and the OEC, two between Cl^- and A-Glu65 and five after the bottleneck at A-Glu65. Other conserved residues proposed to participate in proton transfer [276-278] are located at the channel walls as well, i.e., A-Asp61, D-Glu312, O-Arg178 and O-Asp250 (see Appendix Table 7.7).

In channel D, five water molecules before the first narrow pass when coming from the OEC, two water molecules between the first and second narrow pass and five water molecules after the second narrow pass were modelled. In channel E, six water molecules before and 14 after a narrow pass might be located. In channel F, six water molecules could be assigned before the first narrow pass, three water molecules are located between the first and second narrow pass and nine after the second pass. In channel G, it was possible to model five water molecules in addition to the present chloride ion before and 17 waters after a narrow pass. Radii and amino acids at narrow passes are given in Appendix Table 7.7.

The high number of possible proton channels could be necessary to ensure fast removal of protons from the Mn_4Ca cluster. However, the ability of a channel to transport protons does not only depend on the inscribed water molecules, but also on the presence of protonatable groups with suitable pKa values. In this respect, it is intriguing that many amino acid side chains that have been proposed on the basis of electrostatic calculations to be involved in proton exit pathways [278] are located at the walls of channel C. Of particular